



Proteomic identification of anti-cancer proteins in luteolin-treated human hepatoma Huh-7 cells

Dong Ryeol Yoo, Yun Ho Jang, Yeong Keul Jeon, Ju Yeon Kim, Won Jeon, Yeon Joo Choi, Myeong Jin Nam *

Department of Biological Science, Gachon University of Medicine and Science, 534-2 Yeonsu-dong, Yeonsu-gu, Incheon 406-799, Republic of Korea

ARTICLE INFO

Article history:

Received 26 August 2008

Received in revised form 19 December 2008

Accepted 26 February 2009

Keywords:

Luteolin

Hepatoma

2-DE

ROS

Apoptosis

Peroxioredoxin 6

Prohibitin

ABSTRACT

Luteolin has been shown to exhibit anti-cancer activity against several forms of cancers, including human hepatic cancers. Many in vitro studies have reported anti-oxidant effects of luteolin. Here, we demonstrate using ROS (reactive oxygen species) detection in the human hepatocellular carcinoma cell line, Huh-7, that anti-cancer action of luteolin are mediated through an increasing in intracellular ROS levels. To identify proteins potentially involved in this mechanism, a two-dimensional electrophoresis (2-DE)-based-proteomic approach was employed. Proteomic analysis revealed that several proteins were associated with the anti-cancer effects of luteolin. Interestingly, these proteins included peroxiredoxin 6 (PRDX6) and prohibitin (PHB), which are implicated in ROS metabolism and apoptosis. Western blot analyses confirmed the expression of these proteins in Huh-7 cells following luteolin application. On the basis of these results, we suggest that PRDX6 and PHB are key targets of luteolin that the mechanism of luteolin-induced apoptosis in Huh-7 cells is mediated through effects involving intracellular ROS.

Crown Copyright © 2009 Published by Elsevier Ltd. All rights reserved.

1. Introduction

Hepatocellular carcinoma (HCC) is one of the most fatal forms of malignant human cancers. Treatment options for HCC are extremely limited because the early stages of the disease are difficult to diagnosed, while the later stages have poor prognosis [1]. Although surgery is recommended as the standard treatment option for HCC patients with poor prognosis, post-surgery survival rate is very low [2].

Luteolin is a flavonoid found in tea, fruits, and vegetables [3]. Many studies have shown that luteolin has various biological including anti-inflammatory activity, anti-oxidant properties [4,5], as well as its anti-proliferative activities against various cancer cells [6–12]. Recently, it was shown that luteolin induces apoptosis in the human HCC cell line HepG2 through a mechanism involving mitochondrial translocation of Bax/Bak and activation of c-jun N-terminal kinase (JNK) [8]. Moreover, it has been demonstrated that

luteolin inhibits hepatocyte growth factor (HGF)-induced HepG2 cell invasion, which may be due to downregulation of the MAPK/ERKs and PI3K–Akt pathways [9]. Despite these insights, the biochemical targets of luteolin in HCC cells have not been fully resolved, and the mechanisms underlying the anti-cancer properties remain incompletely understood. In order to facilitate more effective therapeutic approaches, we used two-dimensional electrophoresis (2-DE)-based-proteomic analysis to identify proteins potentially involved in anti-cancer mechanisms of luteolin in the human HCC cell line Huh-7.

Protein expression profiling has improved our understanding of various types of cancer. In studies aiming to elucidate the cellular mechanisms of anti-cancer agents, this technique provides vast information enabling the detection of specific cancer biomarker [13] and the mechanism study of various cancer agents [14]. Here, we performed protein expression profiling of luteolin-treated Huh-7 cells using 2-DE proteomic analysis. Differentially expressed spots were identified and analyzed using matrix-assisted laser desorption/ionization-time of flight mass spectrometry

* Corresponding author. Tel.: +82 32 820 4542; fax: +82 32 816 4542.
E-mail address: genetx@hanmail.net (M.J. Nam).

(MALDI-TOF MS). By using this approach, we detected two proteins, namely, peroxiredoxin 6 (PRDX6) and prohibitin (PHB), which previously have been implicated in ROS metabolism and apoptosis [15–20]. This finding was validated using western blot procedures. On the basis of these results, we suggest that the anti-cancer effects of luteolin are mediated by PRDX6 and PHB through mechanisms involving alterations in ROS metabolism.

2. Materials and methods

2.1. Cell cultures

Human HCC cells Huh-7 were purchased from the Korean Cell Line Bank. Huh-7 cells were maintained in Dulbecco's modified Eagle's medium (Gibco BRL, Grand Island, NY, USA) containing 10% fetal bovine serum (Invitrogen, Carlsbad, CA, USA), penicillin (100 µg/ml) at 37 °C in a 5% carbon dioxide and 95% air humidified incubator. Luteolin was purchased from Sigma (Deisenhofen, Germany). A stock solution of luteolin (100 mM) was prepared in DMSO and stored at –20 °C. Huh-7 cells were plated in 100-mm culture dishes at a density of 5×10^6 cells. As the cells reached 70% confluency, the medium was replaced by a fresh medium containing 200 µM of luteolin. Control cells were cultured in a culture medium containing the same amount of DMSO instead of luteolin.

2.2. Cell proliferation assay

Cells were plated in 96-well plates at a density of 8×10^3 cells per well and incubated for 24 h. The cells were rinsed with PBS and grown in a medium containing various concentrations of luteolin (50, 100, 150, 200 µM). After 24 h (or 48 h) of treatment, the medium was removed and replaced by another medium containing 3-(4,5-dimethylthiazol-2-yl)-2,5-diphenyl-2H-tetrazolium bromide (MTT) solution (1 mg/ml), and the cells were incubated for 2 h at 37 °C. To assess the proportion of viable cells, formazan was solubilized with 150 µl DMSO. Plates were then vortexed at room temperature for 30 min, and the level of formazan was measured using a spectrophotometer at 575 nm.

2.3. DNA fragmentation assay

DNA fragmentation assays were performed to determine whether the anti-cancer activity of luteolin is related to apoptosis. Huh-7 cells (5×10^6) were treated with 0.2% DMSO or various concentrations of luteolin for 24 h. DNA was then obtained using a DNA fragmentation assay kit (Trevigen, Gaithersburg, MD, USA) and loaded on a 1.5% agarose gels. Then, Gels were then stained with 0.5 µg/ml ethidium bromide for 15 min and visualized using a UV transilluminator.

2.4. ROS detection

ROS were detected using fluorescence microscope (Zeiss) and a 5-(and-6)-chloromethyl-2',7'-dichlorodihydrofluorescein diacetate (DCF-DA) probe. Huh-7 cells

(1×10^6) were plated on 60-mm culture dishes and treated with 0.2% DMSO or luteolin (100 µM, 200 µM) for 24 h. After treatment, cells were rinsed with HBSS solution and incubated in a medium containing 20 µM DCF-DA for 15 min at 37 °C in a dark environment. The DCF-DA loaded cells were then rinsed with HBSS solution and observed by using fluorescence microscopy. Fluorescence was measured at an excitation wavelength of 480 nm and an emission wavelength of 520 nm.

2.5. 2-DE

Following 24 h treatment, 5×10^6 Huh-7 cells were harvested and lysed in a lysis buffer (7 M urea, 2 M thiourea, 2% CHAPS, 20 mM DTT, 0.5% Pharmalyte). The lysates were incubated on ice for 1 h and then centrifuged at 14000 rpm for 10 min at 4 °C. After centrifugation, supernatant of the lysates was transferred to a fresh tube. Supernatant protein was then stored at –80 °C for subsequent 2-DE proteomic analysis. Protein concentration was determined using Qubit™ fluorocytometer (Invitrogen, Carlsbad, CA, USA). To investigate the protein expression profiles of controls and luteolin-treated cells, 2-DE proteomic analysis was performed. One hundred micrograms of protein was obtained and diluted in a rehydration buffer (7 M urea, 2 M thiourea, 2% CHAPS, 20 mM DTT, 0.5% Pharmalyte, and 0.002% bromophenol blue) and then loaded on 18-cm IPG strips (pH 3–10, GE healthcare). The rehydration step (12 h) was followed by protein loading. The first dimensional separation was performed using Ettan IPGphor II (GE Healthcare, Korea). Isoelectric focusing (IEF) was performed at 20 °C using the following procedures: 200 V for 1 h, 500 V for 1 h, 1000 V for 1 h, and 8000 V for 3 h. After that, the gel strips were equilibrated for 15 min in an equilibration buffer (6 mol/l urea, 20% glycerol, 2% SDS, and 0.05 mol/l Tris-HCl, with 2% DTT), followed by second equilibration was performed for another 15 min in the same buffer but with 2.5%iodoacetamide to remove excess DTT. For the second dimensional separation, the equilibrated strips were applied on 12.5% SDS-polyacrylamide gels. The SDS polyacrylamide gel electrophoresis (PAGE) was performed in sequence using an Ettan DALT VI system (GE Healthcare), initially at 16 mA per gel for 30 min and then at 24 mA per gel until the dye reached the bottom line of each gel. Polyacrylamide gels were visualized by silver staining to compare spot patterns between control and luteolin-treated cells. Overall, the 2-DE proteomic procedure was performed individually three times for both control and experimental treatments to obtain silver-stained 2-DE gels for image analysis. Differentially expressed protein spots between control and experimental treatments were detected using ImageMaster 2D Platinum (GE Healthcare). Matching of 2-DE gel images was performed using automatic procedure as outlined in the instruction manual.

2.6. In gel digestion

For protein identification, 2-DE gels were stained using coomassie brilliant blue G250 dye (Bio-Rad, Hercules, CA, USA). Differentially expressed protein spots on coomassie

brilliant blue-stained gels that showed a more-than-two-fold change upon image analysis, were identified for subsequent mass spectrometry. These gel spots were transferred to a fresh tube and soaked in 200 mM ammonium bicarbonate for 20 min, after which the supernatant was removed. The gel spot was then rinsed using the following processes: 100% acetonitrile was added to the tube for 1 min and then discarded; 0.1 M ammonium bicarbonate was then put in the tube for 1 min and then discarded. The gel spot was allowed to dry for 10 min. Trypsin solution (10 ng/ μ l trypsin, 50 mM ammonium bicarbonate) was added to the tube for 1 h and then removed. The gel spot was then soaked in 50 mM ammonium bicarbonate for 15 h. Finally, supernatant from the gel spot was transferred to a fresh tube for mass spectrometry.

2.7. Mass spectrometry and protein identification

Mass spectra were obtained using a Voyager-DE STR MALDI-TOF mass spectrometer (Applied Biosystems, Cambridge, MA) with delayed extraction and reflection. The matrix solution was prepared by dissolving 10 mg α -cyano-4-hydroxycinnamic acid in 1 ml of 50% acetonitrile and 0.1% trifluoroacetic acid. The peptide digest (1 μ l) was mixed with 1 μ l matrix solution, and 1 μ l of this mixture was then applied to the stainless steel plate of the mass spectrometer. A matrix peak and a trypsin fragment peak served as internal standards for mass calibration. Following MS processing, proteins were identified by searching the Swiss-Prot database using the MS-Fit search engine from the University of California, San Francisco (UCSF). The mass tolerance was limited to 20 ppm.

2.8. Western blot

Huh-7 cells were treated for 24 h with 100, 200, or 300 μ M of luteolin and then harvested and lysed to prepare the proteins for western blot. Thirty micrograms of protein was loaded on 10% SDS-polyacrylamide gels. Samples were separated using SDS-PAGE at 150 V for 135 min (initial current at 60 mA/gel; end current at 25 mA/gel). Proteins were then transferred electrophoretically to nitrocellulose (NC) membranes with transfer buffer (50 mM Tris, 190 mM glycine, and 10% methanol) at 100 V for 2 h. Blotted membranes were incubated with blocking buffer (50 mM Tris, 150 mM NaCl, 0.1% Tween 20, and 3% skimmed milk) at 24 °C for 1 h. Following three 10-minute treatments in wash buffer (50 mM Tris, 150 mM NaCl, 0.1% Tween 20), membranes were incubated with primary antibodies (anti-peroxiredoxin6 monoclonal antibody from AbCam; anti-prohibitin monoclonal antibody from Calbiochem; and anti- β -actin monoclonal antibody from Sigma as a control for protein loading) for 1 h at room temperature, followed by horseradish peroxidase-labeled secondary antibody for 1 h. The membranes were then washed again and detection was performed using the enhanced chemiluminescence western blot detection system (GE healthcare). Images of each band were analyzed by ImageQuantTL (GE Healthcare) and normalized to β -actin. Representative images of three independent experiments are shown in the results section.

3. Results

3.1. Anti-cancer activity of luteolin upon Huh-7 cells

To quantify the anti-proliferative activity of luteolin upon Huh-7 cells, we performed MTT assays. Time- and dose-dependent cytotoxic effects for luteolin on Huh-7 cells were demonstrated (Fig. 1A). The half maximal inhibitory concentration (IC₅₀) of a 24 h luteolin treatment upon proliferation of Huh-7 cells was approximately 50 μ M. DNA fragmentation assays showed that DNA fragmentation in Huh-7 cells was significantly induced by a 200- μ M treatment with luteolin (Fig. 1B), indicating that apoptotic mechanisms are involved in the anti-proliferative effects of luteolin. In addition, morphological changes in Huh-7 cells were observed following luteolin treatment using phase contrast microscopy (Fig. 1C). Cells showed morphological characteristics of apoptosis, such as chromatin condensation and membrane blebbing, after following treatment.

3.2. Effect of luteolin on intracellular ROS production

Detection of ROS was performed to determine if luteolin-induced apoptosis is mediated by ROS accumulation in Huh-7 cells. Elevated levels of intracellular ROS were found following treatment with increasing concentrations of luteolin (Fig. 2). Accumulation of ROS was significantly induced following treatment with luteolin at 200 μ M for 24 h.

3.3. Comparison of protein expression profiles between control and luteolin-treated Huh-7

Protein expression profiles of Huh-7 cells before and after treatment with luteolin were observed using a 2-DE proteomic analysis. For the image analysis, protein expression profiles of silver-stained 2-DE gels (three from controls and three from luteolin-treated cells) were compared using ImageMaster software. The representative images of silver-stained 2-DE gels are depicted in Fig. 3. Image analysis revealed differential expression of more than 200 protein spots between control and luteolin-treated cells. Sixty-three protein spots showed a greater than two-fold change in density. Twelve of these were subsequently selected for protein identification on the basis of consistently occurring changes in optical density in coomassie brilliant blue-stained 2-DE gels.

Among these spots, eight proteins were down-regulated, while four proteins were up-regulated following luteolin treatment. These spots were identified using MALDI-TOF MS followed by MS-FIT database searches. Proteins were then classified according to their roles in the following functions: DNA synthesis, signal transduction, cell adhesion, RNA transcription, ubiquitination, phosphorylation, transcription regulator, and antioxidation (Table 1).

3.4. Validation of 2-DE results by western blotting

We detected several proteins using 2-DE proteomic analysis, including peroxiredoxin 6 (PRDX6) and prohibitin (PHB), which may mediate anti-cancer effects of luteolin in Huh-7 cell. To confirm the results of 2-DE proteomic analyses, we selected both these proteins for further analysis using western blotting procedures. The PRDX6 and PHB proteins are implicated in ROS metabolism and apoptosis. Western blots revealed that with increasing concentrations of luteolin, PRDX6 expression was increased, whereas PHB expression was decreased (Fig. 4). These findings are consistent with the results of 2-DE proteomic analysis.

4. Discussion

It is well-known that traditional chemotherapy and cancer irradiation-therapy are not as effective for the treatment of HCC compared to other types of cancers, which is likely due in part to difficulties in diagnosing HCC in its early stages [1,2]. Resistance of HCC to treatment is closely related to impairments in apoptosis [21,22], and this is exacerbated as mutated growth regulatory genes accumulate. Therefore, studies seeking to improve HCC treatment

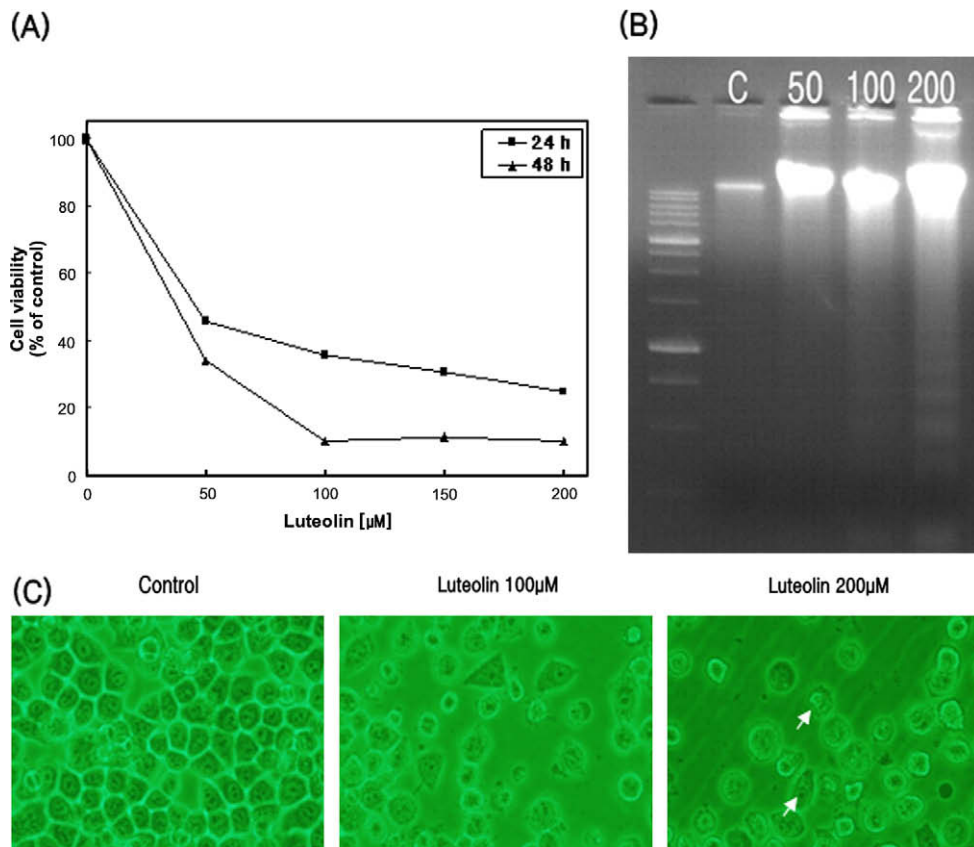


Fig. 1. Anti-cancer activities of luteolin on Huh-7. (A) Cells were treated with various concentrations of luteolin for 24 h or 48 h. Cytotoxicity of luteolin on Huh-7 was assessed using MTT assays. The results showed that luteolin inhibited proliferation of Huh-7 cells in dose- and time-dependent manners. (B) Apoptosis was evaluated by DNA fragmentation assay after cells were treated with various concentration of luteolin (50, 100, 200 μM) for 24 h. This revealed that DNA laddering is significantly induced by 200 μM of luteolin. (C) The morphology of Huh-7 cells was dramatically altered with increasing concentrations of luteolin treatment for 24 h. Morphological characteristics of apoptotic cells, such as chromatin condensation and membrane blebbing, are indicated with arrows. Cells were observed using phase contrast microscopy (400 \times).

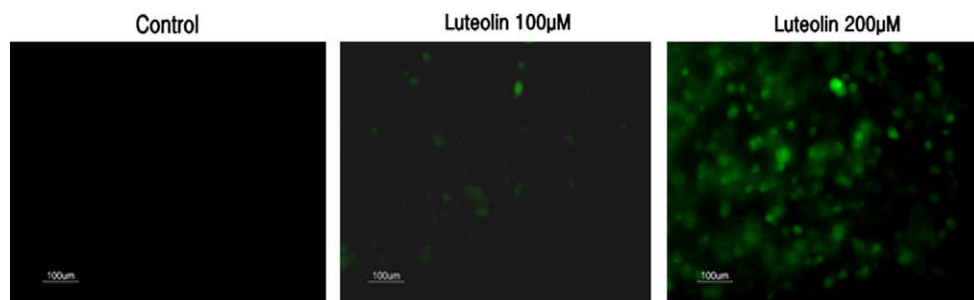


Fig. 2. Effect of luteolin on intracellular ROS production. Huh-7 cells were treated with 100 μM or 200 μM of luteolin for 24 h. Cells were then incubated with 20 μM of DCF-DA for 15 min. Intracellular DCF was detected using fluorescence microscopy. The results show that intracellular ROS levels are significantly increased by 200 μM of luteolin.

strategies should explore how alternative forms of cancer therapy affect molecular mechanisms related to cancer.

Many studies have reported that luteolin inhibits HCC proliferation [7–9]. Some studies have shown that luteolin inhibits proliferation of HCC cell lines including HepG2 (expressing wild-type p53 gene) by cell cycle arrest induced through increased p53 expression [10,11]. Thus,

increased expression of p53 appears to be important in anti-cancer mechanisms of luteolin that involve cell cycle arrest. Further studies reported the anti-cancer effects of luteolin are also related to apoptotic pathways, since typical indicators of apoptosis, such as DNA laddering, chromatin condensation, and membrane blebbing, were observed in several HCC cell lines after luteolin treatment [7,8]

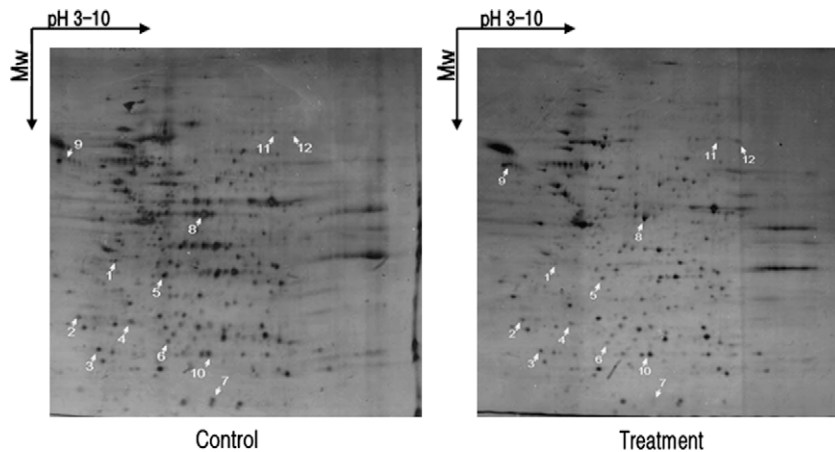


Fig. 3. Protein profiles of control and luteolin-treated Huh-7 cells. Huh-7 cells were treated with 200 μM of luteolin for 24 h. Proteins were separated by pI and molecular weight and visualized by silver staining. Arrows indicate each differentially expressed protein spots between control and luteolin-treated cells. These spots were obtained from coomassie brilliant blue-stained gels and analyzed by MALDI-TOF MS (listed in Table 1).

Table 1

Identification of differently expressed proteins between control and luteolin-treated Huh-7 cells (200 μM luteolin).

Spot no.	Protein name	Protein function	Accession no. ^a	Cov (%)	Theor Mw(Da)/pI	Average fold-change
1	Guanine nucleotide-binding protein G(y) subunit alpha	Signal transduction	P29992	15.0	42124/5.5	-3.84
2	Elongation factor 1-beta	Signal transduction	P24534	29.8	24764/4.5	-2.99
3	Cadherin-7 precursor	Cell adhesion	Q9ULB5	24.3	87060/4.6	-4.14
4	Chloride intracellular channel protein 1	Signal transduction	O00299	28.6	26923/5.1	-3.13
5	Ribonucleotide reductase small subunit	DNA synthesis	P31350	10.9	44878/5.3	-4.31
6	Prohibitin	DNA synthesis	P35232	42.3	29804/5.6	-3.28
7	UPF0258	DNA synthesis	P59773	21.1	12476/6.1	-6.66
8	DNA-directed RNA polymerase III subunit RPC5	RNA transcription	Q9NVU0	12.9	79899/6.1	-5.99
9	Ubiquitin carboxyl-terminal hydrolase 28	Ubiquitination	Q96RU2	18.3	12249/5.1	+2.63
10	Peroxiredoxin 6	Reduces oxidation	P30041	39.7	25035/6.0	+2.69
11	La-related protein 1	Phosphorylation	Q6PKG0	10.5	123511/8.9	+3.28
12	AF4/FMR2 family member 4	Transcription regulator	Q9UHB7	5.3	127460/9.3	+3.93

Cov: Sequence coverage, Theor Mw(Da)/pI: Theoretical molecular weight(Da)/pI, -: down-regulated, +: up-regulated.

^a Swiss-Prot accession number.

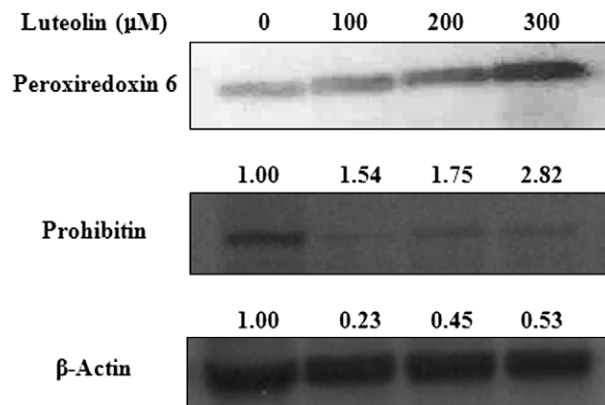


Fig. 4. Effect of luteolin on protein expression of peroxiredoxin 6 (PRDX 6) and prohibitin (PHB) in Huh-7 cells. Cells were treated with various concentration of luteolin for 24 h. The results of western blot experiments show the expression of PRDX 6 is up-regulated while that of PHB is down-regulated with increasing concentrations of luteolin. This is consistent with the results of 2-DE proteomic analyses.

Moreover, some of these investigations revealed possible apoptotic targets of luteolin. Lee et al. [8] showed that luteolin-induced apoptosis in Hep G2 cells (expressing the wild-type p53 gene) is mediated by mitochondrial translocation of Bak/Bax. These authors suggested activation of JNK is an important event in this pathway. However, because a possible mechanism for these effects involves increased expression of death receptor ligands – which were unchanged in that study – this does not explain how the pro-apoptotic action of JNK is involved in luteolin-induced apoptosis. Chang et al. [7] also reported that apoptosis is induced and Bak protein expression is increased after treatment of luteolin in PLC/PRF/5 cells harboring the mutated p53 gene. Therefore, although it is clear that induction of apoptosis is one of the most critical anti-cancer effects of luteolin in both wild-type and mutated p53 cell lines, there may be other apoptotic mechanisms that do not involve altered p53 expression.

In this study, we investigated the anti-cancer activities of luteolin in Huh-7 cells (harboring the mutated p53 gene) to determine if there are alternate apoptotic pathways not involving p53 that may include molecular targets of luteolin. To accomplish this objective, we employed a strategy involving 2-DE-based proteomic analysis. Prior to proteomic analysis, we assessed the level of anti-cancer activity of luteolin in Huh-7 cells using MTT assays, DNA fragmentation assays, and through observation of cell morphological changes (Fig. 1). As concentration of luteolin was increased, cells showed typical characteristics of apoptosis, including DNA laddering, chromatin condensation, and membrane blebbing.

In addition to anti-cancer effects, luteolin is well known as an anti-oxidant [4] in several cancers [23,24] and cancer cells [25,26]. It has been shown that the anti-cancer activity of luteolin is mediated by scavenging ROS. However, several studies have raised questions regarding the anti-oxidant activities of flavonoids [27,28]. Min et al. [28] showed that flavonoids act as anti-oxidants at low concentration (0.1 μM), but they also demonstrated that some flavonoids (usually at high concentration: >100 μM), including luteolin, exhibit pro-oxidant activities on Calf thymus DNA under certain conditions. These findings led us to investigate the level of intracellular ROS in control and luteolin-treated cells (Fig. 2). Our findings indicate that luteolin can act as a pro-oxidant in Huh-7 cells, which may subsequently induce apoptosis.

To identify molecular components related to these effects, 2-DE proteomic analysis was performed. This showed the significant differences in protein expression profiles between luteolin-treated and control cells (Fig. 3). We chose 12 spots showed dramatic changes (more than twofold) in intensity following image analysis and then identified these spots using MALDI-TOF-MS (Table 1). Interestingly, several proteins such as PRDX6 and PHB are regarded as ROS- and apoptosis-related proteins. The results of the 2-DE proteomic analysis were validated using western blot procedures.

PRDX6 is a member of the PRDX family, associated with functions such as cell proliferation, differentiation, and apoptosis [15–17]. According to their peroxidase activity mechanisms, PRDXs are classified as either 1-Cys PRDX or 2-Cys PRDXs. The only member of 1-Cys PRDX is PRDX6,

and the effects of PRDX6 are related to both GSH peroxidase and phospholipase A2 activity [29]. Many studies have suggested that the over-expression of PRDX6 in cells of various tissues, especially the liver, is associated with protection of cells from cellular oxidative stresses [30]. These studies further suggested that PRDX6 functions in anti-oxidant defense mainly by facilitating repair of damaged cell membranes via reduction of peroxidized phospholipids [16,30]. In this study, we demonstrated increased expression of PRDX6 in Huh-7 cells following treatments with increasing concentrations of luteolin. On the basis of DCF fluorescence observations, ROS production seems to be an important event of luteolin-mediated apoptosis. In addition, it is wellknown that increased PRDX6 expression is related to the level of intracellular ROS [15]. Therefore, we suggest that mechanisms of luteolin-mediated anti-cancer activity in Huh-7 are closely related to increased ROS levels, accompanied by over-expression of PRDX-6. These insights led us to consider the function of PHB in the anti-cancer effects of luteolin.

PHB, an evolutionarily conserved protein with homologues found in species ranging from yeast to man is located in the inner membrane of the mitochondria and appears to be a reliable marker of mitochondria integrity that is essential for cell survival [19]. In keeping with its name, PHB has been suggested to inhibit cell proliferation through apoptosis and cell cycle arrest involving increased p53 expression [19]. However, the anti-proliferative activity of PHB is controversial, because other studies showed the opposite effects of PHB in apoptosis [20,31,32]. Consistent with previous studies, we demonstrate here decreased expression of PHB in Huh-7 cells combined with increased apoptosis. Thus, we focused on the alternative PHB pathway, which does not involve Rb- and p53-related anti-proliferative effects of PHB (Rb and p53 were mutated in Huh-7). The alternative effects of PHB in Huh-7 cells might be related to the mutated form of Rb and p53. Our research on alternative pathways revealed that the decline in PHB levels may be associated with the accumulation of damage resulting from mitochondrial oxygen radicals [33,34]. Some studies have reported that oxygen radicals are generated because of high luteolin concentrations [28] and subsequently induce DNA damage. This result is consistent with our DCF fluorescence observations, which showed that luteolin triggered an increased intracellular production of ROS. Therefore, we suggest that PHB down regulation is closely related to luteolin-mediated apoptosis, induced by increased ROS levels.

In conclusion, although some studies have reported anti-oxidant activities of luteolin [23–26] we suggest that ROS production is an important event in luteolin-mediated apoptosis in Huh-7 cells. In keeping with this, it is noteworthy that other studies have also reported pro-apoptotic behavior of luteolin, induced by luteolin-mediated oxidative stress [27,28]. The pro-oxidant activities of luteolin might explain the changes in expression of PRDX6 and PHB. We propose that mechanisms of luteolin-mediated anti-cancer effects in Huh-7 cells are closely related to increased ROS production involving changes in expression of PRDX6 and PHB.

Conflicts of Interest Statement

None declared.

References

- [1] M.A. Feitelson, B. Sun, N.L. Satiroglu Tufan, J. Liu, J. Pan, Z. Lian, Genetic mechanisms of hepatocarcinogenesis, *Oncogene* 21 (2002) 2593–2604.
- [2] K.X. Xue, Molecular genetic and epigenetic mechanisms of hepatocarcinogenesis, *Ai Zheng* 24 (2005) 757–768.
- [3] H. Matsuda, H. Cai, M. Kubo, H. Tosa, M. Iinuma, Study on anti-cataract drugs from natural sources. II. Effects of buddlejae flos on in vitro aldose reductase activity, *Biol. Pharm. Bull.* 18 (1995) 463–466.
- [4] J.E. Brown, H. Khodr, R.C. Hider, C.A. Rice-Evans, Structural dependence of flavonoid interactions with Cu²⁺ ions: implications for their antioxidant properties, *Biochem. J.* 330 (Pt 3) (1998) 1173–1178.
- [5] G. Galati, M.Y. Moridani, T.S. Chan, P.J. O'Brien, Peroxidative metabolism of apigenin and naringenin versus luteolin and quercetin: glutathione oxidation and conjugation, *Free Radic. Biol. Med.* 30 (2001) 370–382.
- [6] Q. Zhang, X.H. Zhao, Z.J. Wang, Flavones and flavonols exert cytotoxic effects on a human oesophageal adenocarcinoma cell line (OE33) by causing G2/M arrest and inducing apoptosis, *Food Chem. Toxicol.* 46 (2008) 2042–2053.
- [7] J. Chang, Y. Hsu, P. Kuo, Y. Kuo, L. Chiang, C. Lin, Increase of Bax/Bcl-XL ratio and arrest of cell cycle by luteolin in immortalized human hepatoma cell line, *Life Sci.* 76 (2005) 1883–1893.
- [8] H.J. Lee, C.J. Wang, H.C. Kuo, F.P. Chou, L.F. Jean, T.H. Tseng, Induction apoptosis of luteolin in human hepatoma HepG2 cells involving mitochondria translocation of Bax/Bak and activation of JNK, *Toxicol. Appl. Pharmacol.* 203 (2005) 124–131.
- [9] W.J. Lee, L.F. Wu, W.K. Chen, C.J. Wang, T.H. Tseng, Inhibitory effect of luteolin on hepatocyte growth factor/scatter factor-induced HepG2 cell invasion involving both MAPK/ERKs and PI3K-Akt pathways, *Chem. Biol. Interact.* 160 (2006) 123–133.
- [10] B. Plaumann, M. Fritsche, H. Rimpler, G. Brandner, R.D. Hess, Flavonoids activate wild-type p53, *Oncogene* 13 (1996) 1605–1614.
- [11] S.B. Yee, J.H. Lee, H.Y. Chung, K.S. Im, S.J. Bae, J.S. Choi, N.D. Kim, Inhibitory effects of luteolin isolated from *Ixeris sonchifolia* Hance on the proliferation of HepG2 human hepatocellular carcinoma cells, *Arch. Pharm. Res.* 26 (2003) 151–156.
- [12] M.E. Schutte, M.G. Boersma, D.A. Verhallen, J.P. Groten, I.M. Rietjens, Effects of flavonoid mixtures on the transport of 2-amino-1-methyl-6-phenylimidazo[4,5-b]pyridine (PhIP) through Caco-2 monolayers: an in vitro and kinetic modeling approach to predict the combined effects on transporter inhibition, *Food Chem. Toxicol.* 46 (2008) 557–566.
- [13] P.R. Srinivas, M. Verma, Y. Zhao, S. Srivastava, Proteomics for cancer biomarker discovery, *Clin. Chem.* 48 (2002) 1160–1169.
- [14] V.E. Bichsel, L.A. Liotta, E.F. Petricoin 3rd, Cancer proteomics: from biomarker discovery to signal pathway profiling, *Cancer J.* 7 (2001) 69–78.
- [15] V.L. Kinnula, P. Paakko, Y. Soini, Antioxidant enzymes and redox regulating thiol proteins in malignancies of human lung, *FEBS Lett.* 569 (2004) 1–6.
- [16] Y. Manevich, A.B. Fisher, Peroxiredoxin 6, a 1-Cys peroxiredoxin, functions in antioxidant defense and lung phospholipid metabolism, *Free Radic. Biol. Med.* 38 (2005) 1422–1432.
- [17] A.B. Fisher, C. Dodia, K. Yu, Y. Manevich, S.I. Feinstein, Lung phospholipid metabolism in transgenic mice overexpressing peroxiredoxin 6, *Biochim. Biophys. Acta* 1761 (2006) 785–792.
- [18] L.G. Nijtmans, S.M. Artal, L.A. Grivell, P.J. Coates, The mitochondrial PHB complex: roles in mitochondrial respiratory complex assembly, ageing and degenerative disease, *Cell Mol. Life Sci.* 59 (2002) 143–155.
- [19] G. Fusaro, P. Dasgupta, S. Rastogi, B. Joshi, S. Chellappan, Prohibitin induces the transcriptional activity of p53 and is exported from the nucleus upon apoptotic signaling, *J. Biol. Chem.* 278 (2003) 47853–47861.
- [20] S. Mishra, L.C. Murphy, B.L. Nyomba, L.J. Murphy, Prohibitin: a potential target for new therapeutics, *Trends Mol. Med.* 11 (2005) 192–197.
- [21] X.Y. Dong, X.W. Pang, S.T. Yu, Y.R. Su, H.C. Wang, Y.H. Yin, Y.D. Wang, W.F. Chen, Identification of genes differentially expressed in human hepatocellular carcinoma by a modified suppression subtractive hybridization method, *Int. J. Cancer* 112 (2004) 239–248.
- [22] X.X. Duan, J.S. Ou, Y. Li, J.J. Su, C. Ou, C. Yang, H.F. Yue, K.C. Ban, Dynamic expression of apoptosis-related genes during development of laboratory hepatocellular carcinoma and its relation to apoptosis, *World J. Gastroenterol.* 11 (2005) 4740–4744.
- [23] M.J. Wu, C.L. Huang, T.W. Lian, M.C. Kou, L. Wang, Antioxidant activity of *Glossogyne tenuifolia*, *J. Agri. Food Chem.* 53 (2005) 6305–6312.
- [24] G. Seelinger, I. Merfort, U. Wolffe, C.M. Schempp, Anti-carcinogenic effects of the flavonoid luteolin, *Molecules* 13 (2008) 2628–2651.
- [25] K. Horvathova, L. Novotny, A. Vachalkova, The free radical scavenging activity of four flavonoids determined by the comet assay, *Neoplasma* 50 (2003) 291–295.
- [26] M. Ruweler, A. Anker, M. Gulden, E. Maser, H. Seibert, Inhibition of peroxide-induced radical generation by plant polyphenols in C6 astrogloma cells, *Toxicol. In Vitro* 22 (2008) 1377–1381.
- [27] T.S. Chan, G. Galati, A.S. Pannala, C. Rice-Evans, P.J. O'Brien, Simultaneous detection of the antioxidant and pro-oxidant activity of dietary polyphenolics in a peroxidase system, *Free Radic. Res.* 37 (2003) 787–794.
- [28] K. Min, S.E. Ebeler, Flavonoid effects on DNA oxidation at low concentrations relevant to physiological levels, *Food Chem. Toxicol.* 46 (2008) 96–104.
- [29] Y. Manevich, S.I. Feinstein, A.B. Fisher, Activation of the antioxidant enzyme 1-Cys peroxiredoxin requires glutathionylation mediated by heterodimerization with pi GST, *Proc. Natl Acad. Sci. USA* 101 (2004) 3780–3785.
- [30] Y. Manevich, T. Sweitzer, J.H. Pak, S.I. Feinstein, V. Muzykantov, A.B. Fisher, 1-Cys peroxiredoxin overexpression protects cells against phospholipid peroxidation-mediated membrane damage, *Proc. Natl. Acad. Sci. USA* 99 (2002) 11599–11604.
- [31] G. Fusaro, S. Wang, S. Chellappan, Differential regulation of Rb family proteins and prohibitin during camptothecin-induced apoptosis, *Oncogene* 21 (2002) 4539–4548.
- [32] J. Fellenberg, M.J. Dechant, V. Ewerbeck, H. Mau, Identification of drug-regulated genes in osteosarcoma cells, *Int. J. Cancer* 105 (2003) 636–643.
- [33] A. Sharma, A. Qadri, Vi polysaccharide of *Salmonella typhi* targets the prohibitin family of molecules in intestinal epithelial cells and suppresses early inflammatory responses, *Proc. Natl. Acad. Sci. USA* 101 (2004) 17492–17497.
- [34] P.W. Piper, D. Bringloe, Loss of prohibitins, though it shortens the replicative life span of yeast cells undergoing division, does not shorten the chronological life span of G0-arrested cells, *Mech. Ageing Dev.* 123 (2002) 287–295.